Agent-based modelling of southward coastal migration by humpback whale mother–calf pods off eastern Australia

Jasper de Bie [1,2,3,4,*] , Serena B. Lee [1,2,3,4], Jan-Olaf Meynecke [1,2,3,4], Elisa Seyboth [5], Saumik Samanta [6], Marcello Vichi [7,8], Alakendra Roychoudhury [6], Brendan Mackey [1,2]

[1] Griffith Climate Action Beacon, Griffith University, Gold Coast, Queensland, Australia

[2] Whales & Climate Research Program, Griffith University, Gold Coast, Queensland, Australia

[3] Coastal and Marine Research Centre, Griffith University, Gold Coast, Queensland, Australia

[4] Cities Research Institute, Griffith University, Gold Coast, Queensland, Australia

[5] Mammal Research Institute Whale Unit, Faculty of Natural and Agricultural Sciences,

University of Pretoria, Pretoria, South Africa

[6] Department of Earth Sciences, Stellenbosch University, Stellenbosch, South Africa

[7] Marine and Antarctic Research Centre for Innovation and Sustainability (MARIS),

University of Cape Town, Cape Town, South Africa

[8] Department of Oceanography, University of Cape Town, Cape Town, South Africa

*Correspondence to : Jasper de Bie, Coastal and Marine Research Centre, Griffith University, G51 Room 2.14, Gold Coast, Qld 4222, Australia. Email: j.debie@griffith.edu.au

ABSTRACT

Humpback whales *Megaptera novaeangliae* encounter a variety of environmental conditions during seasonal migration between feeding grounds and breeding grounds. Relationships between environmental conditions and migratory movements are largely unknown due to a lack of oceanographic data coincident with their presence/absence. We begin to address this knowledge gap by developing a new agent-based modelling (ABM) approach designed to predict southward migration of mother–calf (MC) pairs along a stretch of the east Australian coast between the Great Barrier Reef (GBR) and Gold Coast (GC) bay, which includes a known resting area, Hervey Bay (HB). To assess our ability to reproduce observed migration patterns, numerical experiments were undertaken in which static (bathymetry) and dynamic (currents, sea surface temperature) variables between August and October 2017 governed movements. These experiments revealed how bathymetry influences HB usage, and a necessity to apply different directionality preferences to whales before and after negotiating HB, which appear to closely align with coastline orientation. The ABM provides a novel, suitable framework for simulating MC humpback whale migration, and an important first step in the development of predictive models of humpback whale behavior. Developing such tools is increasingly necessary to predict how changing ocean conditions are likely to affect their distribution.

Keywords: agent-based model; behavior; cetacean; Megaptera novaeangliae; migration

1 INTRODUCTION

A range of environmental factors, both abiotic (e.g., bathymetry, temperature) and biotic (e.g., predation pressure), are known to influence migratory patterns and behaviors in marine animals (Allen et al., 2018; Shaw, 2016). Among these drivers, ocean currents are responsible for heat and nutrient transport and thereby playing a crucial role in providing food, transport, and suitable habitat for resident species and migratory species such as whales and turtles (Bestley et al., 2019; Hays, 2017; Wilson et al., 2016). Along the East Coast of Australia, oceanic conditions are predominantly driven by the East Australian Current (EAC), which flows southward after splitting off the South Equatorial Current upon reaching the Great Barrier Reef (GBR) (Brinkman et al., 2002; Ceccarelli et al., 2013; Ridgway & Dunn, 2003). The EAC separates from the coast at approximately 32°S and feeds into an offshore eddy field (Oke et al., 2019). The EAC is responsible for heat transport toward the pole and influences the local climate and marine ecosystems (Malan et al., 2020, 2022; Suthers et al., 2011; Xie et al., 2021).

The East-Australian subpopulation (E1) of humpback whales, *Megaptera novaeangliae*, inhabits the coastal area several months of the year: The southern region of the GBR is utilized for breeding and calving during austral winter (Smith et al., 2012) before the coastal part of their southward migration progresses until the region offshore Eden (New South Wales) is reached. Trajectories from tagged humpback whales suggest they then continue to travel to Antarctica via Tasmania or New Zealand through deep waters, mainly using Area V during the summer feeding season (Andrews-Goff et al., 2018; Johnson et al., 2022) before making the same journey back to the GBR. Humpback whale migration typically takes place in separate cohorts depending mostly on age and reproductive status (Craig et al., 2003; Stevick et al., 2003). These cohorts consist of mother–calf (MC) pairs, mature females without a calf, immature whales, or mature males. Females with or without calf may be escorted by one or more males for short periods of time, but interactions with other MC pods are very scarce (Craig et al., 2003; Franklin et al., 2011; Ransome et al., 2022). Migration to the feeding grounds starts with females without a calf leaving the breeding grounds, followed by immature whales, adult males, and finally MCs. The delayed migration of the MC is so the calf has grown the strength to migrate and survive its first feeding months in cold, polar waters (Dawbin, 1966, 1997). The return migration is initiated by the MC cohort such that they spend the least amount of time in such an extreme environment. Females without a calf, or those already pregnant, leave the feeding ground last. Differences in migratory timing ensure the cohorts reach breeding and feeding grounds at times that coincide with the presence of calm and warm waters required for breeding activities or an abundance of prey species, respectively (Burns et al., 2014; Chittleborough, 1965; Dawbin, 1956, 1997).

Despite their migration covering vast distances over months, humpback whales, on average, return to the same breeding and feeding grounds at roughly the same time every year with limited exchange between populations and substocks (Baker et al., 2013; Schmitt et al., 2014). The foundation for their migration route is likely provided through social learning, with fidelity to both breeding and feeding grounds transmitted from mother to calf during the first year (Baker et al., 2013). However, this mechanism does not provide all the necessary

information required to navigate accurately over such long distances, as the migration route can vary from year to year due to changes in oceanographic conditions. Instead, an appropriate behavioral response to local environmental conditions is required. It is less clear what geophysical cues drive their decision-making process and the more detailed route selection (Horton et al., 2020; Horton, Hauser, et al., 2017). Recently, Meynecke et al. (2021) assessed current knowledge about the relationships between humpback whales and environmental conditions. Relevant information on factors influencing migration is limited, but indicates that humpback whales prefer shallow coastal waters, while seamounts and underwater ridges may aid in navigation through deep waters (Meynecke et al., 2021). The role of sea surface temperature (SST) is considered to be minor during migration; however, breeding grounds with high temperatures (>28°C) are unlikely to attract individuals (Rasmussen et al., 2007), and avoidance of such high temperatures may persist during southward migration.

The lack of detailed knowledge on humpback whale behavior during migration or over prolonged periods of time stems from challenges with data collection related to their spatial range, residency in remote areas, and short surface intervals (Hunt et al., 2013; Nowacek et al., 2016). In the absence of long-term data sets, or given inconsistently collected data, numerical models have been proven suitable to fill out gaps (Meynecke et al., 2021). For instance, correlative machine learning models such as Maxent can be applied using presence-only data to predict suitable breeding habitat for humpback whales (e.g., Derville et al., 2018; Smith et al., 2012). When it comes to modelling direct whale responses to fine-scale, spatially and temporarily varying environmental conditions, agent-based models (ABMs) (also called individual-based models) are needed that can adequately capture the decision-making process and its effects over classic population-modelling approaches (DeAngelis & Diaz, 2019). Essentially, these involve an explicit representation of an individual (or some functionally related group of organisms)—referred to as the "agents"—and how they react to local environmental conditions based on a set of behavioral rules. The individual decisions of a large number of agents can reveal emergent patterns at the population level. ABMs have been used frequently for simulating movement patterns of migrating animals (e.g., elk, *Cervus elaphus*, Bennett & Tang, 2006; blue whales, *Baleanoptera musculus*, Dodson et al., 2020; pink-footed geese, *Anser brachyrhynchus*, Duriez et al., 2009; and salmon smolts, *Oncorhynchus keta*, Goodwin et al., 2006). Recently, Guarini and Coston-Guarini (2022) presented an ABM for humpback whale migration on a global scale. Using an ethogram describing each agent's daily activity, combined with an index representing its perception of an environmental gradient based on latitude, the authors showed that migration patterns between feeding and breeding grounds could be simulated. However, behavioral responses to dynamic environmental variables were not included and proposed by the authors as possible ways for improvement. Furthermore, migratory movements on the continental shelf (depth <200 m) were designed to prevent stranding rather than reflecting the species' strong preference for these depths during the coastal part of their migration (Meynecke et al., 2021).

Understanding the movement patterns of humpback whales and relevant environmental factors that may influence them is important for their conservation management in the face of growing climate change and other human pressures (Meynecke et al., 2020; Tulloch et al., 2019). Taking the above limitations into consideration, the aims of this modelling were to describe the development and functionality of an ABM for simulation of the southward

coastal migration of Breeding Stock E1 humpback whales and to present preliminary results. The behavioral rules that underlie movements by the agents were derived from the assessment of the relevant literature and involve the incorporation of static (bathymetry) and dynamic (SST and currents) variables at scales suitable for movements close to shore. Each agent represented one unit of the MC cohort, in simulations. The functioning of the model was validated through comparison with previously published satellite tracking data along the East Coast of Australia (Gales et al., 2010).

2 METHODS

2.1 Study area

The Australian GBR is the world's largest coral reef ecosystem, extending from far northeast of Queensland to the Bunker group of islands just north of Hervey Bay (hereafter HB), over a distance of ~2300 km (Figure 1). The GBR consists of a variety of individual reefs, islands, and coral cays, providing a unique area of biodiversity and national and international importance. Water depth throughout is mostly shallow (<50 m) except for the outer reefs and continental shelf boundary. While humpback whales are occasionally sighted as far north as Port Douglas (16.48° S, 145.46° E), the southern part of the GBR, particularly the lagoon waters between the Whitsunday Islands and Broad Sound (~20°S to ~22°S), is an important wintering ground (Smith et al., 2012). This was taken into account when determining the model domain for this study, with the northern boundary set at 20.0°S latitude. The southern boundary was set to 28.6°S latitude, at the Queensland/New South Wales border (Figure 1), which falls within the region covered by the hydrodynamic model (see Section 2.2).

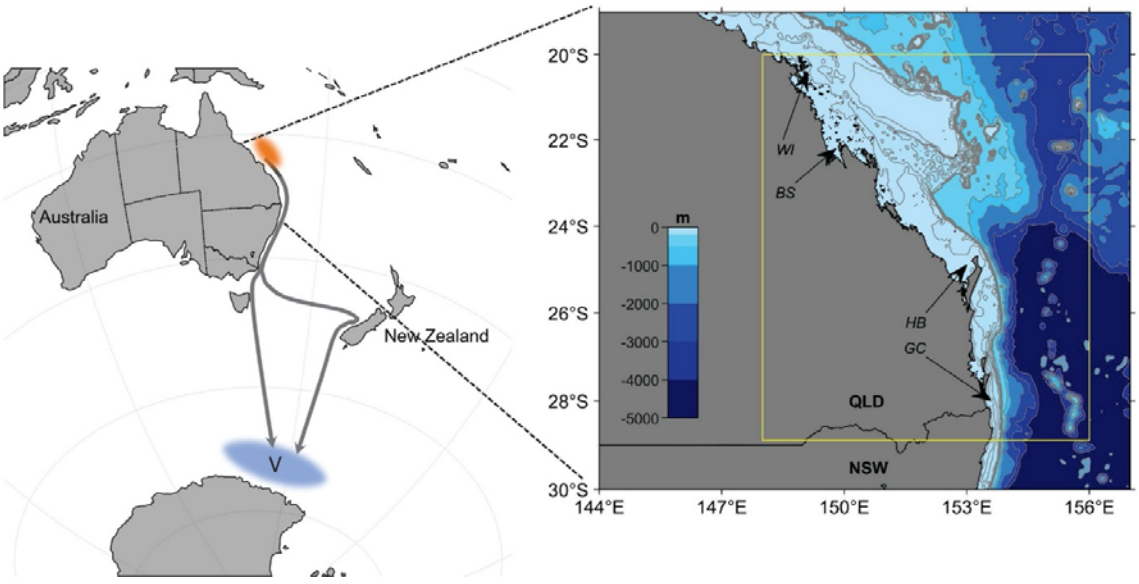

FIGURE 1. Schematic of parts of Oceania and Antarctica with the southward migration route of E1 humpback whales from the Great Barrier Reef (GBR) breeding ground (orange shading) to feeding Area V (blue shading) indicated by dark gray arrows. The inset shows parts of Queensland (QLD) and New South Wales (NSW) with the domain used in ABM simulations indicated by a yellow rectangle. Blue shading and gray contour lines follow bathymetry levels extracted from the ETOPO1 relief model. State borders are denoted by black lines. The black arrows indicate the locations of the Whitsunday

Islands (WI), Broad Sound (BS), Hervey Bay (HB), and the Gold Coast (GC), respectively. ABM, agent-based modelling.

2.2 Environmental data input

Ocean model data were extracted from the *eReefs* platform (https://ereefs.org.au/ereefs), which has been under development since 2012, that integrates and couples hydrodynamic (including tides), sediment, and biogeochemical models for the entire GBR (Steven et al., 2019). It provides users with environmental simulation of past, present, and future conditions within the GBR. To simulate circulation driven by both regional and global circulation processes, the GBR 4-km resolution hydrodynamic model (GBR4) was forced at open boundaries by outputs from the 10-km resolution Ocean Modelling Analysis and Prediction System (OceanMAPS) model and in turn provided information to the 1-km resolution hydrodynamic model (GBR1) close to the coast. Further details on *eReefs* components, functionality, calibration, and accessibility are presented in Steven et al. (2019). In this study, hourly *eReefs* model outputs were obtained for a spatial domain extending from 20°S to 29°S and 148°E to 155°E, and for a period of 3 months (August 1, 2017 to November 1, 2017). These months typically represent the southern humpback whale migration and sufficient swim speed data were available for the selected study year. Principal parameters extracted from *eReefs* included zonal and meridional surface currents (u and v, hereafter u_{flow} and v_{flow}), and SST from the top layer, which represent averaged conditions over the upper 1.5 m of the water column. Spatial plots of monthly (August, September, and October) mean values of u_{flow}, v_{flow}, and SST were produced in Matlab® 2023a. Bathymetry data across the same spatial domain were extracted from the high-resolution depth model for the GBR (Beaman, 2017), which represents a blended bathymetry/elevation data set with approximately 30 m spatial resolution, spanning the coastal region from Cape York to northern New South Wales (10°S–29°S, 142°E–156°E).

2.3 Behavioral rule development

2.3.1 Movement and swim speed

In the ABM, each agent represented one unit of the MC cohort (i.e., a mother with calf migrating pod). This cohort was selected due to the availability of the most reliable swim speed estimations for it, as well as their utilization of HB for resting purposes (see Section 2.3.2). An agent's movement in the ABM consisted of a contribution of the local flow field and its own swim speed. The 2-D flow vectors (u_{flow}, v_{flow}, in meter per second) were interpolated from the dynamic *eReefs* environment to each agent's location at every hourly timestep. The mean swim speed of each agent was also determined and renewed every timestep. This value was drawn from a Gaussian distribution of speeds with mean ± SD = 3.80 ± 1.77 km hr^{-1}, which were derived from swim speeds of humpback whales from the MC cohort observed on the Gold Coast (GC). MC pods were followed by whale-watching vessels, and the start and end locations as well as the vessel's track duration were used for calculations (H. Kela, personal communication). The mean swim speed can then be decomposed into its x- and y-components if angle ϑ, which represents directionality, is known. As whales were predominantly moving southward during the simulation period, this angle can be assumed to be close to 180°, and analysis of the average bearing from

trajectories of tagged humpback whales along the east coast (Andrews-Goff et al., 2018) has confirmed this to be an adequate assumption. Thus, the directionality for each agent was drawn from a Gaussian distribution of angles around 180° ± 20° (σ_ϑ) and, if applicable, renewed every timestep. The resultant volitional swim vector (u_{swim}, v_{swim}, in meter per second) was added to those of the flow to update the coordinates (x_t, y_t) at time t from the previous position (x_{t-1}, y_{t-1}) after time increment (Δt, in seconds) as:

$$X_t = X_{t-1} + (u_{swim} + u_{flow}) \bullet \Delta_t \quad (1)$$

$$Y_t = Y_{t-1} + (v_{swim} + v_{flow}) \bullet \Delta_t \quad (2)$$

Behavioral rules described below influence the directionality and thereby the swim speed component of each agent.

2.3.2 Resting

HB is an area used in humpback whale migration as an important resting or stopover site for over a third of the stock (predominantly females and calves), which stay in the bay for 1.4–2 weeks (Chaloupka et al., 1999; Franklin et al., 2014; Franklin et al., 2018). Due to its geometry, HB acts as a "funnel" and individuals must swim north to move around Fraser Island before continuing their southward migration (Figure 1). During this stay period, the whales are predominantly resting (McCulloch et al., 2021), which is of little interest to simulating their migratory movements. Resting inside of HB was thus included in the models through the following process (Figure 2, top section; Figure 3a):

- Whenever an agent passes through a predefined rectangular polygon close to the entrance of HB (pink rectangle, Figure 3a), it is assigned a 40% chance it will "enter" HB for resting, reflecting the aforementioned part of the stock that does so.
- If the agent does not enter HB, it is placed outside and continues migration south and is not attributed a stopover in HB.
- If the agent enters HB, its residence time is randomly set, which varies between 10 and 14 days; the agent is placed at an arbitrary inside location for this duration, then being moved to a location outside to continue its migration.

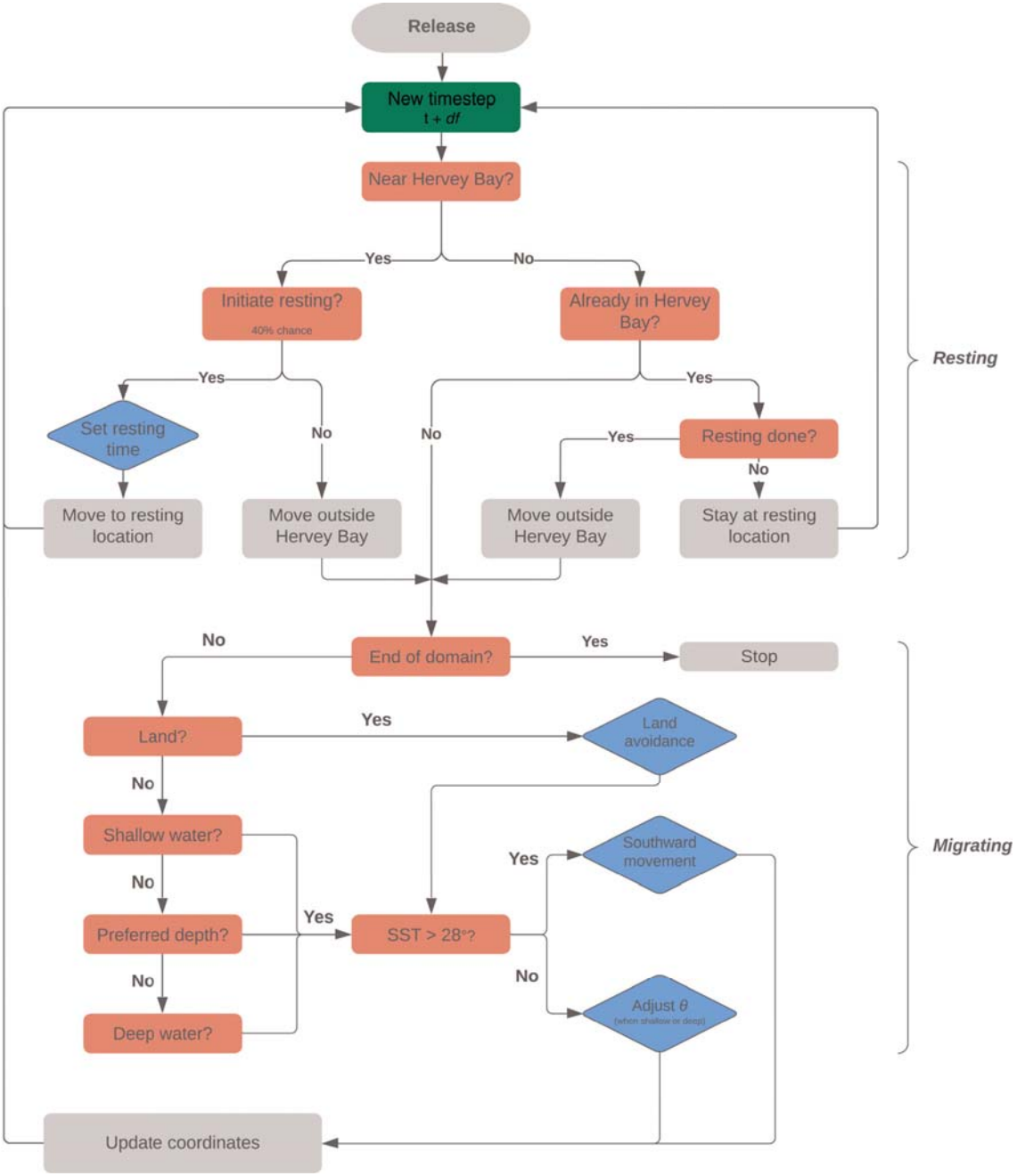

FIGURE 2. Schematic of the process flow used in the agent-based model. Red boxes denote location or environment assessment, blue boxes denote responses, and gray boxes denote actions. ϑ denotes the mean directionality of an agent (MC pod). At every timestep after release (green box), the location of each agent was assessed: If near Hervey Bay, the resting process was applied; otherwise, the agent was migrating, and the local environment was assessed with associated decision-making (see main text). New coordinates were subsequently calculated and a new timestep initiated, repeating this process until all agents reached the end of the domain or 3 months had passed.

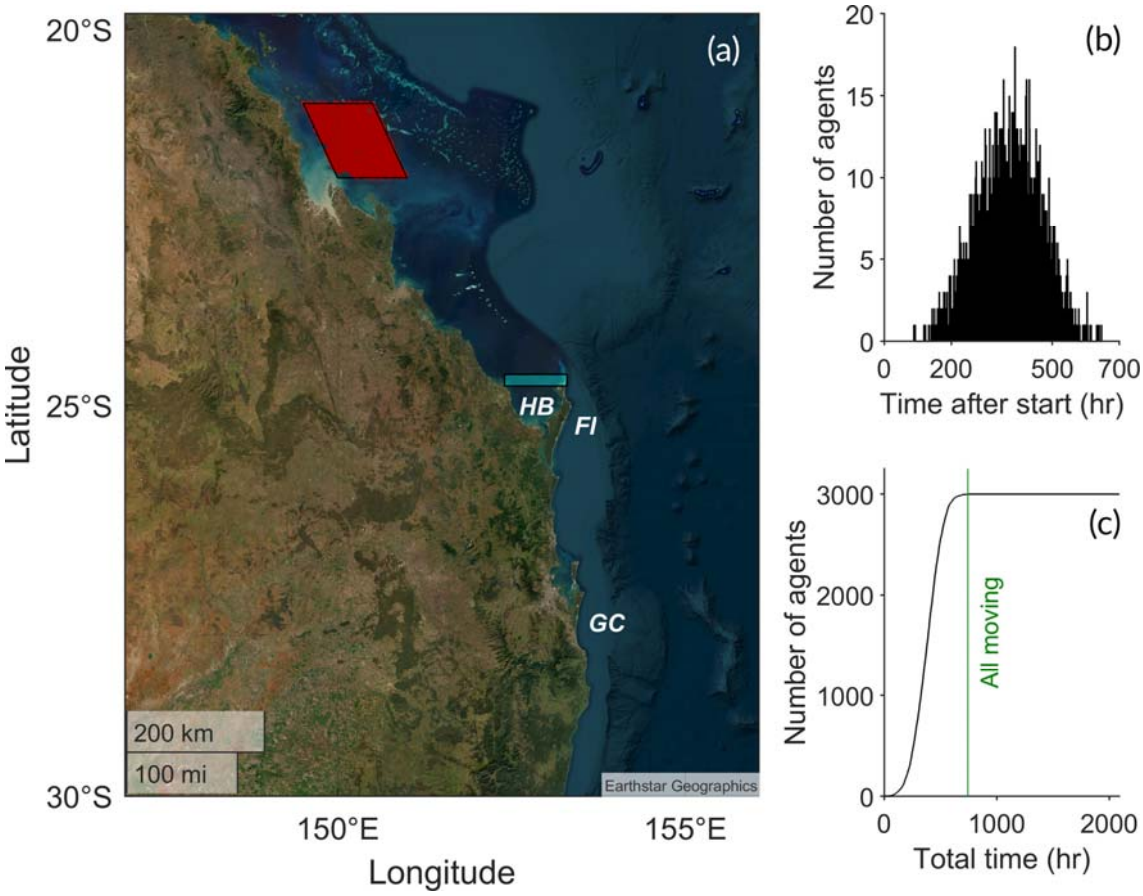

FIGURE 3. Example of initialization stage of the agent-based model. (a) Plan view of the model domain with the black parallelogram indicating the release area and red dots within denoting the starting location of 3,000 agents. Starting bathymetries were between 20 and 200 m. Cyan rectangle shows where the Hervey Bay (HB) resting process was evaluated. Fraser Island (FI) forms the eastern boundary of HB. Simulations continued until all agents reached the Gold Coast (GC) bay. (b) Example of the distribution of the release of agents over a 31-day period (744 h). (c) Number of agents in the model showing all were moving after August 31 (green vertical line) and remained in the domain until the end of the period being analyzed (November 1), although not moving south of GC.

Through this approach, migration is believed to be adequately captured for all agents. Further south, the GC has been recognized as a resting area with residence times less than in HB (1–3 days based on fluke matches but not fully known; Valani et al., 2020), thus not being incorporated in the current development of the ABM.

2.3.3 SST response

While higher SST values may be tolerated, most humpback whale breeding grounds are restricted to SST values below 28°C (Rasmussen et al., 2007). It can be assumed that an aversion to similar high SST values holds during migration; moreover, these are unlikely to be encountered during their southward migration into colder waters. However, an absence of whales in high SST waters does not provide information on their behavioral response when encountering certain values, which is required for the ABM. SST is known to be one of the factors driving HW decision-making at the small scale (Reinke et al., 2016) and likely at the

larger scale as well. Detailed information on the decision-making process itself is unavailable from the current literature, but it can be assumed that unwanted conditions must trigger a behavioral response, leading to the whales initiating movement elsewhere. Here, this process was deemed an avoidance response. When an agent encountered an SST >28°C, the avoidance response was triggered resulting in continuation of southward movement, thus without adjusting directionality ϑ (Figure 2, bottom section). This was very likely to represent a movement toward water with a lower SST compared to the current location and kept southward migration dominating (as opposed to adjusting ϑ to induce movements onshore or offshore or to the north).

2.3.4 Land avoidance and bathymetry response

Similar to the SST behavioral response, the known preference of the species for shallow waters of the continental shelf during migration (Kavanagh, Noad, et al., 2017; Meynecke et al., 2021) was represented in the ABM by an evaluation of the bathymetry of the agent's current location (Figure 2, bottom section). Three main depth threshold values were used, denoting either "land" or water too shallow for a whale to be found in (D_{Land}, 15 m), "shallow" water ($D_{shallow}$, 30 m), or "deep" water (D_{deep}, 200 m). This created four zones that trigger behavioral land avoidance ($D < D_{land}$), or a bathymetry behavioral response to shallow ($D_{land} < D < D_{shallow}$), preferred ($D_{shallow} < D < D_{deep}$) or deep water ($D > D_{deep}$). When water was too shallow or too deep, avoidance was triggered by adding or subtracting a trigonometric 10° increment (ϑ_{adjust}) to ϑ for a more offshore and onshore directionality, respectively. Essentially, the agent's movements over the course of an hourly timestep were gradually directed toward water of preferred depth. When in water of preferred depth, no such directional change was made. An agent can get into water that was too shallow or on land, due to updating positions at the end of a previous timestep. As a proxy for land avoidance, in this case, the original trajectory that led to this position was reevaluated with the same swim speed but with different values for ϑ (in 10° increments) and the most offshore point was kept. The SST and bathymetry behavioral response at the alternative point was then evaluated as per the above. If no good alternative point was found (essentially, the agent was at a dead end in this situation), the location at the previous timestep was kept and movement was reassessed at the next timestep, when a new swim speed was applied, and environmental conditions were updated and evaluated (except bathymetry).

2.4 Model setup and analysis

The ABM was designed and coded using Matlab 2023a. It consisted of separate scripts for generating release locations, running simulations, and analyzing the outcomes. Agents were released (i.e., had their start position for the southward migration) in an area that resembled their wintering ground in the GBR (Smith et al., 2012), represented as a parallelogram bounded between 21°S–22°S, and 149.5°E–151°E (Figure 3a). Due to the presence of shallow reefs and islands, bathymetry can be too shallow ($D < D_{land}$) in the release area, which would trigger unrealistic land avoidance behavior directly after release. To overcome this, a total of 10,000 starting coordinates that fell within the release area were randomly generated and their associated bathymetry evaluated. From these, 3,000 locations where $D_{land} < D < D_{deep}$ were kept and used as potential starting locations for each of the agents used in simulations.

Annually, the first southward migrating humpback whales of the breeding season are usually sighted in the stopover site (HB) during the month of August (Franklin et al., 2011), during which local whale-watch operators start their activities. Therefore, the release of agents was chosen to take place over the month of August 2017. The number of agents that entered the model per hourly timestep was chosen to follow a Gaussian distribution, meaning the bulk of the population started migrating around mid-August (Figure 3b). After all agents have started their movements, they remained in the model until the end of simulations (3 months, Figure 3c) as it was computationally more efficient to retain them rather than removing them after reaching the GC. Instead, their final locations in the GC used for analysis were kept constant until simulations were complete.

The script used for running simulations enabled the specification of certain parameters and pre-allocated a data structure that allowed storing each agent's attributes during migration. For each agent, initial input consisted of only the *x*- and *y*-coordinates and bathymetry of its release location. The script iterated through each hourly timestep with associated *eReefs* data loaded in, processing the actions of each agent during each of these. At every timestep after release, the location of each agent present in the model was assessed to determine whether it was in/near HB and thereby subject to resting (see Section 2.3.2). If not, an agent was considered migrating, in which the local environment was assessed (land, then SST, then bathymetry) with associated decision-making (Figure 2). For each agent, new coordinates were subsequently calculated and output (e.g., coordinates, bathymetry, SST, u_{flow}, v_{flow}) stored. During the first month of simulations, new agents entering the model were added at the end of a timestep. After that, each new timestep repeated the above for each agent until they reached the end of the domain, or the 3 months had passed. The final output was stored for analysis.

The success of a single simulated migration was defined as the percentage of whales that left the GBR area, reached HB, and then reached GC. The outcome of each simulation was further evaluated through several metrics, which were calculated from the trajectory of each agent, allowing for a meaningful comparison between different simulations. These metrics included (i) the values for SST encountered before and after HB (SST_{HB}, SST_{GC}); (ii) the time from release to reaching the HB rectangle (T_{HB}), and from the outside of HB to GC (T_{HBGC}) to provide temporal quantification of the stage of migration before and after encountering HB; and (iii) the bathymetries encountered by agents before and after encountering HB (D_{HB}, D_{HBGC}) to provide information on depth use during migration.

To identify the areas of relatively higher density of agents during migration, the 3 months of simulation time were divided into two-weekly periods, and the number of agents within certain distance of each grid point was calculated and binned for each period. For visualization purposes, a 12-km distance (~.1°) was chosen here. Binned numbers were then used to create spatial scatter plots for selected simulations using “geoscatter” in Matlab 2023a. This approach counts individuals within each 2-week timeframe more than once for different locations but, in doing so, highlights the preferred routes taken by most agents as opposed to simply visualizing each separate path that would obscure this trend.

To provide further insight into how migration depended on input parameters, a sensitivity analysis around the values for ϑ, and ϑ_{adjust}, D_{land}, $D_{shallow}$, and D_{deep} was performed (Table 1).

Used values for D_{land} included 15, 20, 25, 30, and 35 m, with a consistent distance of 15 m maintained between D_{land} and $D_{shallow}$. Based on these values, groups of simulations were assigned a capital letter (A-E, respectively) and each single simulation was assigned a number (1–12), reflecting values for ϑ, ϑ_{adjust}, and D_{deep}. For instance, simulation "A1" had corresponding values for D_{land} = 15 m, $D_{shallow}$ = 30 m, ϑ = 180°, ϑ_{adjust} = 10°, and D_{deep} = 200 m. Decreasing the value for ϑ to 160° (± 10°) imposed a south easterly directionality toward the continental shelf edge, whereas increasing ϑ_{adjust} to 20° and 30° strengthened the avoidance response. When varying the value for D_{land}, starting locations in water of sufficient depth in the GBR were generated accordingly. Overall, 60 different sensitivity scenarios were tested, each simulating the movements of 3,000 agents (Table S1).

TABLE 1. Parameters and associated values used in the agent-based model for migrating humpback whales from the mother–calf (MC) cohort along the East Coast of Australia.

Parameter	Symbol	Value	Other values explored
Agents			
Mean swim speed[a]	V_{mean}	3.80 km h^{-1}	
Standard deviation of swim speed[a]	σ_V	1.77 km h^{-1}	
Mean directionality	ϑ	180°	160°
Standard deviation directionality	σ_ϑ	20°	
Adjustment angle of directionality	ϑ_{adjust}	10°	20, 30°
Environment			
Land detection threshold[b]	D_{land}	15 m (A simulations)	20, 25, 30, 35 m (B, C, D, and E simulations)
Shallow water detection threshold	$D_{shallow}$	30 m	35, 40, 45, 50 m
Deep water detection threshold	D_{deep}	200 m	150 m
Maximum SST detection threshold	SST_{max}	28°C	
Time			
Time step	dt	1 hr	

Abbreviation: SST, sea surface temperature.

[a] H. Kela, personal communication.

[b] A consistent distance of 15 m between D_{land} and $D_{shallow}$ was used.

2.5 Validation

In 2009, researchers from the Australian Antarctic Division (AAD) successfully deployed satellite tags (N = 13) on northward migration humpback whales off the coast of Evans Head, NSW. After spending the breeding season in the GBR, whales migrated southward again, some of which still had the tag attached. Details of the tagging procedure are available in Gales et al. (2010). These deployments represent the only data set with relevant movement

tracks through the model domain used in simulations and have previously been used as validation data for the identification of the GBR breeding habitat (Smith et al., 2012). Matlab 2023a was used for the visualization of the trajectory of one relevant individual and compared to the outcome of simulations.

3 RESULTS

Mean values of u_{flow} showed consistent patterns between all 3 months of simulations across the model domain (Figure S1). The highest positive values (eastward) were in the northern part, reaching up to .8 m s^{-1}. Conversely, values in the release area and toward GC varied between −.2 and .2 m s^{-1}, corresponding to up to 19% of an agent's mean swim speed (3.80 km hr^{-1}≈1.06 m s^{-1}). Mean values of v_{flow} varied between .4 (northward) and −1.0 m s^{-1} (southward) across the model domain with consistent spatial patterns each month (Figure S2). Maximum southward velocity components were notably present in the offshore region between HB and GC, approaching the magnitude of an agent's swim speed. In contrast, mean v_{flow} in the release area and toward HB varied between 0 and −.2 m s^{-1} (approximately 19% of an agent's swim speed).

Mean SST values were below the 28°C threshold across most of the domain in August and September, while areas in the north and close to shore had SST values close to the threshold in October (Figure S3). The highest SST value encountered by any agent was 27.4°C (A8, Table S1). Between the GBR and HB, higher values for SST were under A simulations, ranging between 26.6 and 27.4°C, over 1.5°C higher than the maximum SST encountered under any of the other simulations. Between HB and GC, encountered values for SST did not differ much between simulations, ranging between 23.7 and 25.6°C (Table S1). Altogether, none of the SST values were above the 28.0°C threshold that would induce an SST-related response in movements, meaning further results can be described solely in terms of bathymetry encountered, directionality, and its adjustment angle.

The percentage of agents that left the GBR and entered the HB polygon was near 100% under the B (D_{land} = 20 m, $D_{shallow}$ = 35 m) and C (D_{land} = 25 m, $D_{shallow}$ = 40 m) simulations, but less under the others (Figure 4a). Under the A simulations (D_{land} = 15 m, $D_{shallow}$ = 30 m), this varied between 66.2% and 100%, while this dropped from 100% to .6% under the D simulations (D_{land} = 30 m, $D_{shallow}$ = 45 m). Under D simulations, the release location of ≤.1% of the agents was surrounded by water too shallow to allow for movement; thus, not all agents left the GBR and migrated southward. Under E simulations (D_{land} = 35 m, $D_{shallow}$ = 50 m), the percentage of agents entering the HB polygon ranged from 0% to 18.1% (Table S1). Under B–E simulations, 100% of agents that started migration reached GC within the 3 months, but not under the A simulations, where this varied between 65.1% and 99.9% (Table S1).

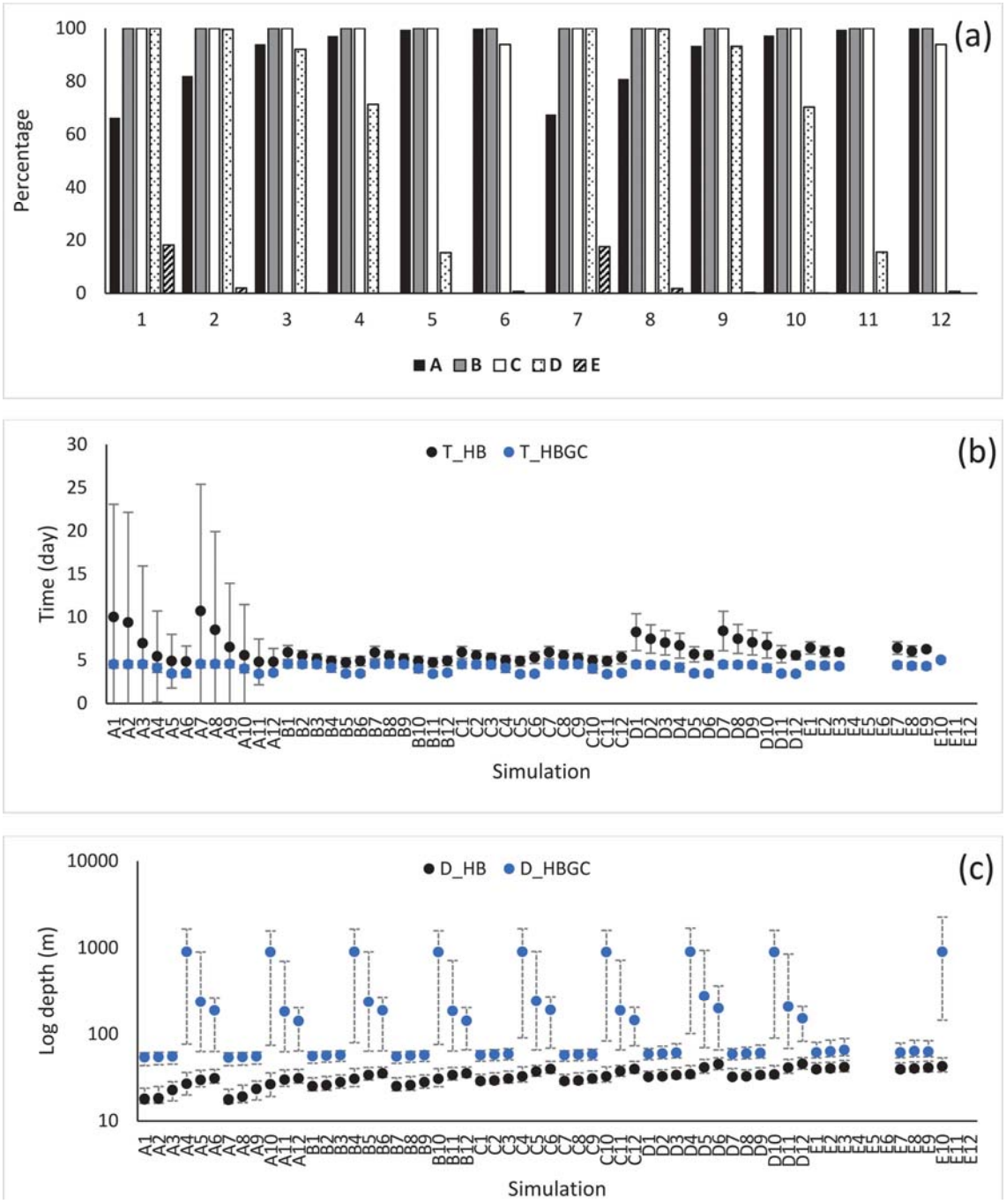

FIGURE 4. Results from agent-based model simulations. (a) Percentage agents reaching the HB polygon after release in the GBR under simulations A–E with settings denoted by the number on *x*-axis (Table S1). For example, A1–E1 and A12–E12 are shown first and last, respectively. (b) Mean (± SD) time in days taken by successful agents to reach HB (black) and subsequently GC (blue). (c) Median log depth (m) encountered by successful agents between release and HB (black) and between HB and GC (blue), with 25th and 75th percentiles depicted as dashed lines. GBR, Great Barrier Reef; GC, Gold Coast; HB, Hervey Bay; SD, standard deviation.

Under A simulations with $\vartheta = 180°$, the agents predominantly utilized areas close to the shoreline, and as a result, many ended up in the very shallow waters of inlets and bays before reaching HB due to land avoidance, which resulted in highly variable values for T_{HB}, up to 10.68 ± 14.72 days (Figures 4b and 5a). Due to these delays, many agents were still scattered throughout the domain by the end of simulations (purple circles, Figure 5a). Both increasing the directionality and adjustment angle resulted in movements and utilization of areas further offshore with associated higher values of median bathymetries. This reduced delay, and many more agents reached HB by mid-September, and almost 100% of agents reached HB in 4.80 and 4.83 days for simulations A6 and A12, respectively (Figure 4b). However, not all agents had reached GC by the end of October and utilized deep water regions south of HB (Figure 5f). Mean T_{HBGC} of agents that reached the HB polygon successfully was not affected by changing D_{deep} and decreased from 4.54 to 3.42 days when directionality and adjustment angle increased (Figure 4b). Agents from B or C simulations utilized areas slightly further offshore and were no longer delayed in their transit time to HB, reaching it by mid-September and subsequently GC by the second week of October (Figure 5b,c). Values of T_{HB} by agents were very similar between these simulations (Figure 4b), with highest values when $\vartheta = 180°$ (mean between 5.16 and 5.90 days) compared with when $\vartheta = 160°$ (mean between 4.74 and 5.30 days). A combination of $\vartheta = 160°$ and $\vartheta_{adjust} = 30°$ resulted in higher densities of agents further offshore before reaching HB around the same period, and similarly, higher densities in deeper waters south of HB before reaching GC mostly by the end of September (Figure 5g,h). Under C simulations, an increase in ϑ_{adjust} led to agents not reaching the HB polygon (.7% and 6% for $\vartheta_{adjust} = 20°$ or 30°, respectively), as they avoided the shallow entrance and subsequently moved past HB (Figure 5h). Mean T_{HBGC} of agents that entered the HB polygon was not affected by altering D_{deep}, with lower values for $\vartheta = 160°$. It ranged between 3.37 and 4.56 days with lower values resulting from an increase in both directionality and adjustment angle (Figure 4b; Table S1). Agents from D simulations started to avoid the shallower waters inside of the GBR release area and utilized routes further offshore toward HB. Regions with high densities of agents were generally further offshore compared to A–C simulations, but successful agents reached HB slightly later (last 2 weeks September; Figure 5d). This was caused by the now-too-shallow area near the HB entrance, resulting in limited routes available into the polygon. Agents that reached the HB polygon took longer to find this route, with T_{HB} values ranging from 8.38 ± 2.28 days to 5.56 ± .49 days (Figure 4b). Regardless of D_{deep}, the number of agents reaching the HB polygon decreased with increasing ϑ_{adjust}. This effect was more pronounced with $\vartheta = 160°$, with only 19 and 18 agents reaching the HB polygon for $D_{deep} = 200$ m and 150 m, respectively (D6 and D12; Table S1; Figure 5i). Mean T_{HBGC} of agents that entered the HB polygon took between 3.41 and 4.49 days to reach GC and were faster when directionality was set to 160°. T_{HBGC} was similar regardless of changing D_{deep} (Figure 4b). Under E simulations, the areas utilized by agents the most after release were the furthest offshore, and because of this, the number of agents that successfully reached the HB polygon in September was lowest (Figure 5e; Table S1). The western part of the release area was too shallow for any agents to follow, and most agents either followed the eastern part of the release area, or areas further offshore. Reducing the value of D_{deep} had little to no effect on bathymetries and T_{HB} (Table S1). Changing ϑ to 160°, agents utilized areas past the HB polygon and avoided this altogether on their way to reaching GC early September (Figure 5j). Only two agents reached the HB polygon out of all simulations with this setting (E10; Table S1). Successful agents took a maximum of 6.42 ± .70 days to reach the HB polygon when $\vartheta = 180°$ and $D_{deep} = 200$ m, reducing this variable to 150 m made no

difference. After HB, agents took a maximum of 4.40 ± .39 days to reach the GC when ϑ = 180° and D_{deep} = 200 m, and 4.40 ± .39 days when D_{deep} = 150 m (Figure 4b).

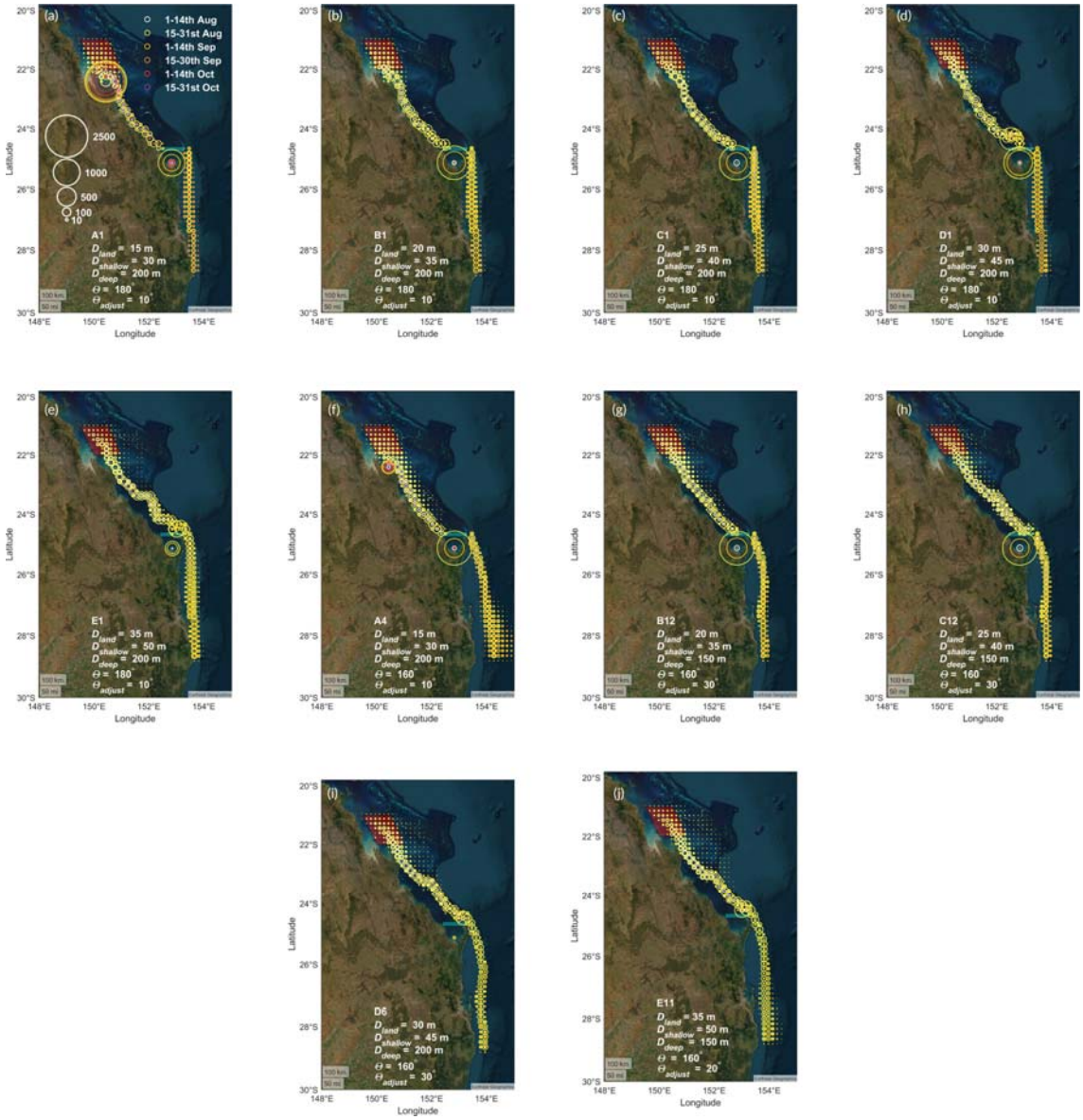

FIGURE 5. Two-weekly density plots of 3,000 agents representing migrating E1 humpback whales after leaving the Great Barrier Reef (GBR, red parallelogram), entering or passing by the Hervey Bay (HB) polygon (cyan rectangle), and subsequently reaching the Gold Coast (GC) at 28.5°S. Panel (a–j) show binned (12 × 12 km) densities from one specific simulation with name and relevant parameter settings used in each shown at the bottom. Legends of the size and color scale of circular markers are shown in panel (a) and apply to all.

Under A simulations, median bathymetries encountered before HB ranged from 18 to 31 m with maximum values of 86 m. Decreasing directionality had a noticeable effect on D_{HBGC}, with median values increasing to over 200 m (A4, A5, and A10; Figure 4c). While a higher adjustment angle pushed the agents closer to shore *enroute* to GC, thus decreasing median D_{HBGC}, the maximum values experienced by agents exceeded 4000 m under A simulations

(Table S1). Under B and C simulations, median D_{HB} did not exceed 40 m with highest bathymetry 119 m (Figure 4c; Table S1). Median D_{HBGC} was between 55 and 59 m when directionality was southward but increased dramatically when directionality set to 160° (maximum of 905 m). Similar to A simulations, decreasing the adjustment angle resulted in lower median D_{HBGC} encountered, ranging between 143 and 244 m (Figure 4c) as avoidance to deep water was stronger. Maximum values for D_{HBGC} exceeded 4,000 m under B and C simulations (Table S1). Under D simulations, median D_{HB} did not exceed 45 m (Figure 4c), with maximum values reaching 300 m (Table S1). Median D_{HBGC} was lower when directionality was southward (ranging between 59 and 61 m) than when this was set to 160° (ranging between 153 and 901 m), while increasing the adjustment angle lowered median D_{HBGC} under these simulations to values near 200 m (Figures 4c and 5i). Maximum values for D_{HBGC} again exceeded 4,000 m under D simulations (Table S1). Under E simulations, median D_{HB} did not exceed 42 m, with a maximum value of 79 m. Median D_{HBGC} was between 61 and 66 m with southward directionality and D_{deep} 150–200 m and ϑ_{adjust} between 10° and 30° (Figure 4c). Maximum values for D_{HBGC} ranged between 252 and 1387 m and decreased with increasing ϑ_{adjust} (Table S1). The two successful agents under any E simulation with $\vartheta = 160°$ were too few to analyze their encountered conditions in terms of bathymetry and transit times further.

Based on all simulation results (Table S1), the most successful ones were those with D_{land} values of 20 and 25 m (B and C simulations, respectively), as most agents reached the HB polygon without delay in shallow coastal water or avoidance to the entrance altogether.

Tagging data from the AAD showed some individuals initiating southward migration within the GBR, including one that migrated all the way south again (#88754). This individual started southward migration on July 19 at an estimated location that is covered by the release area used in simulations. It travelled in a southeasterly direction, did not enter HB, and subsequently moved southward passing GC on August 11 (Figure 6). The movements of this individual north of HB agreed with areas of high agent density resulting from simulations with $\vartheta = 160°$ (Figure 5h–j). Movements south of HB matched simulations with $\vartheta = 180°$ very well (Figure 5a–e).

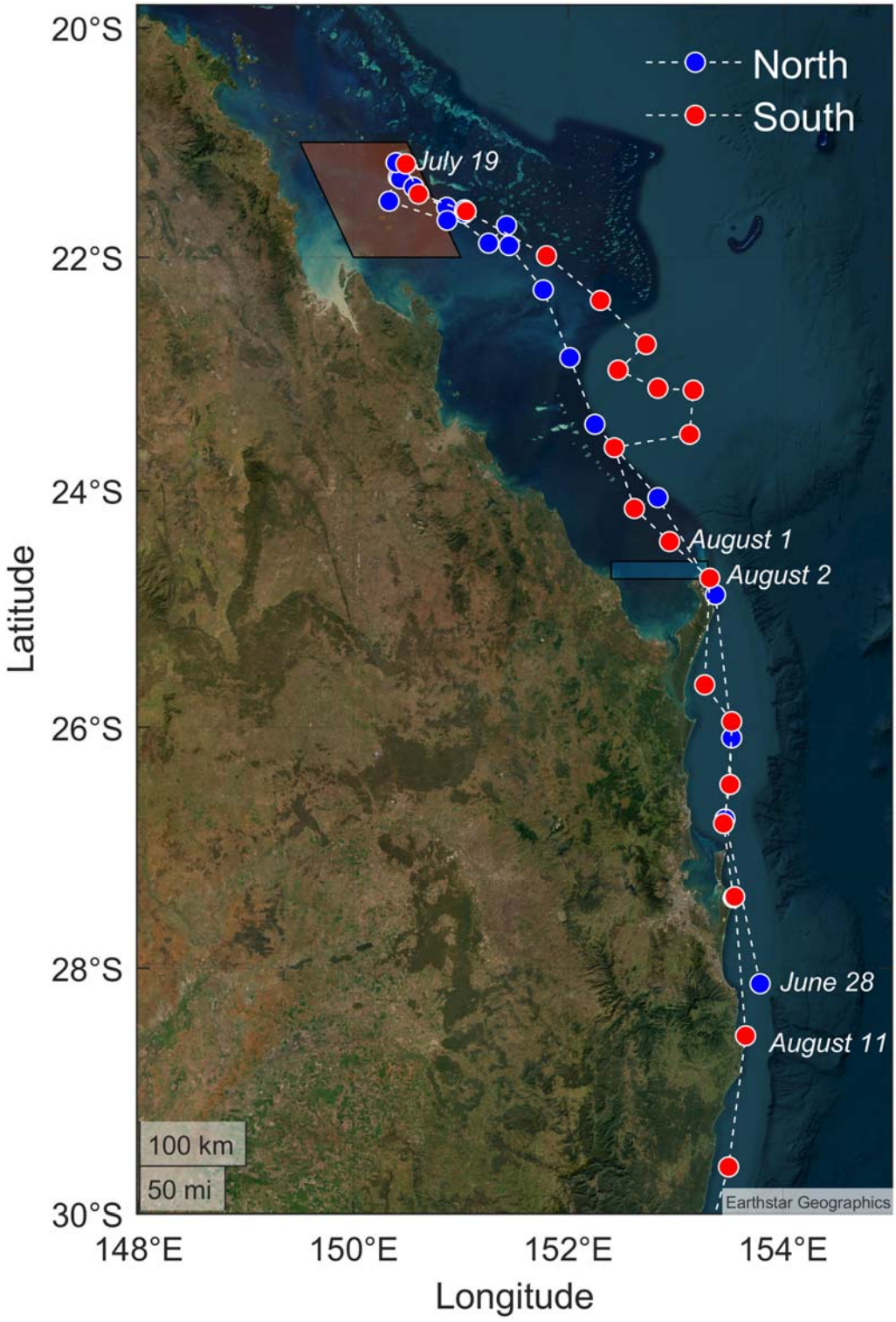

FIGURE 6. Route taken by a tagged humpback whale (#88754) that completed both northward (blue) and southward (red) migration in 2009. Several locations are shown with timestamps, including date of tagging on June 28 and southward migration starting on July 19. Release area in the GBR and HB are denoted by an orange parallelogram and blue rectangle, respectively. The tagged whales' underlying data courtesy of the Australian Antarctic Division, and previously published (Gales et al., 2010; Smith et al., 2012). GBR, Great Barrier Reef; HB, Hervey Bay.

4 DISCUSSION AND CONCLUSIONS

Here, we present the first ABM for migrating humpback whales, in which both static (bathymetry) and dynamic (currents, SST) environmental variables are used by agents to govern movements. Applied to the coastal migration of the MC cohort of the East-Australian subpopulation (E1), we show that the ABM can adequately capture partial southward migration. In its current version, it can act as a framework for further investigation into the factors that determine decision-making during the migration of humpback whales and possibly other species.

We developed the ABM for a two-dimensional case, using only environmental data from the top layer of the ocean. Imposing an appropriate horizontal swim speed on each agent in the ABM is essential for capturing reliable migration times for the entire cohort. Noad and Cato (2007) reported migration speeds over 15 km hr^{-1} for a single singing (a form of mating display) male and over 23 km hr^{-1} for a group of nonsinging whales of the E1 population; however, due to the presence of a calf, the MC pair migrates slower compared to other cohorts (Chittleborough, 1953; Noad & Cato, 2007). The agents' swim speeds used here (mean ± SD = 3.80 ± 1.77 km hr^{-1}) were obtained from citizen science data collected for southward migrating MC pods in the GC in 2017. These values are similar to those reported elsewhere in the literature. For instance, Cusano et al. (2020) reported swim speeds of 3.56 ± 1.86 km hr^{-1} for E1 MC pods during southward migration, and Riekkola et al. (2018) reported swim speeds of 3.1 ± 1.5 km hr^{-1} for migrating MC pods from the E/F populations. To account for individual differences between swim speeds, we added variation by determining a new value for every agent, at every timestep.

A response to SST was not found in our simulations, as agents always encountered values below 28°C. As agents travel southward into colder water, this is not surprising, but they could have encountered this in the GBR near the release area (Govekar et al., 2022). In the ABM, the SST response (i.e., to travel southward without adjusting directionality) is similar to the bathymetry response when an agent is within the preferred range. Since median D_{HBGC} values are predominantly in the preferred range with ϑ~180° across simulations (Figure 4b), agents stay mostly within this range, and thus, this response is functioning as intended. By extension, the SST response would also work as intended if water with SST > 28°C was encountered. While this response did not affect the current outcomes of simulations, it is a valuable component of the framework and its effects may be investigated in future versions of the ABM, applied to migration patterns further north (Garrigue et al., 2015) or under climate conditions that are associated with warmer waters (e.g., La Niña events).

As the depth-associated value for land avoidance increased from 15 to 35 m, the offshore paths with highest densities of agents increased as expected, and this effect was amplified by decreasing directionality from 180 to 160°. However, when the depth-associated value for land avoidance was 30 or 35 m, the number of agents entering the HB polygon dropped, as avoidance of such depths excluded them from entering the shallow HB area. This suggests bathymetries up to 25 m must be in the preferred range for this cohort to enter HB for resting purposes. Beyond HB, a directionality of 160° “pushed” agents into much deeper water than when they travelled in the southward direction, often with median bathymetry values close to that of the continental shelf boundary of approximately 200 m. With southward

directionality, median bathymetries were around 60 m across simulations, slightly higher than what was recorded in the GC for MC pairs (mean 33 m; Valani et al., 2020), but likely the result of some agents travelling through deeper waters and not directly returning to preferred range by deep water avoidance. The maximum value for adjustment angle was 30° here, and while this could be increased (e.g., 45°), the result reduces median bathymetry and creates zigzag trajectories that are unlikely to be an adequate representation of real migratory movements.

There is little detailed information on the routes taken by E1 humpback whales during their southward migration, making validation of the simulated trajectories a challenge. However, relevant spatial information is available from the 2009 satellite tag data set (Figure 6). While limited to just a single female individual, the trajectory of this tagged whale (#88754) shows a south-easterly route taken until HB followed by a clear southward route to GC. Based on this, simulations in which a directional shift after HB is included could possibly capture migration patterns as observed in the wild for these humpback whales. The trajectory further shows similar paths taken northward and southward, an interesting feature that may be addressed in simulations focusing on E1 humpback whales travelling to breeding grounds. Temporal information from the tagged whale is not directly comparable to the calculated transit times, as this individual was without a calf and started migration before the MC cohort. However, there is no evidence that besides the timing of migration, the route taken differs between cohorts; therefore, the paths taken by this tagged whale can be assumed to resemble those of the MC cohort.

There are several justifications for posing a behavioral change in direction after negotiating HB. First, migrating humpback whales show high route fidelity despite changing oceanic conditions suggesting they use geophysical cues for decision-making and course changing along the way (Horton et al., 2020). Second, besides SST and bathymetry, there are other environmental variables influencing humpback whale distribution during migration. One of these factors is the “distance to shore” (e.g., Viddi et al., 2010), which would be relatively constant throughout the domain when imposing a directional change from HB onward. Third, along parts of the model domain south of HB, the EAC transports warm water southward (Figure S2) and E1 humpback whales have been shown to make use of coastal (thermal) fronts associated with this current for navigation (Reinke et al., 2016). This would prevent humpback whales from going far offshore, but this may not necessarily result in them taking a route very close to shore.

Under the most successful simulations (B and C), median transit times between release and HB were between 4 and 7 days, and agents took between 3 and 5 days to reach GC after HB. Agents had typically also reached the GC by the end of September. The transit times are very difficult to validate with field data as data collection north of HB is scarce, and due to a lack of tagging data from individuals moving southward along this part of the domain. In addition, the simulated transit times are influenced by differences in swim speed, environmental conditions encountered, and starting location in the release area. Between 2010 and 2020, sightings data collected on the GC have confirmed the presence of southward migrating MC pods in August and September, similar to most simulations' output, but lasting until the end of October (H. Kela, personal communication, Torre-Williams et al., 2019, Valani et al., 2020). In rare cases, a mother and calf pair can be easily tracked if one of them has a clear identifiable characteristic. During 2021, a newborn calf with a lower jaw deformity could be followed

southward by means of photographs by the public. It was last sighted in HB on September 9, and 14 in Point Arkwright and resighted in the GC on the 18th. While there is no evidence that the calf started migrating south on the 9th, and still would have had to swim around Fraser Island, its transit time to reach Port Arkwright after exiting HB was at least 4 days. This calf (while likely being slowed down due to its handicap) still took longer than estimated by the outcome of the most successful simulations.

Based on the above evidence, albeit limited, our simulations thus may have underestimated transit times, for which there are a few explanations. First, there may be a difference between the daytime and nighttime swim speed of humpback whales, which can have a noticeable effect on migration time as this slows or speeds up movements for several hours each night. To date, however, research into diel patterns of humpback whale ecology has revealed changes in singing (Au et al., 2000; Ross-Marsh et al., 2021; Shabangu & Kowarski, 2022) and feeding (Friedlaender et al., 2013; Parks et al., 2014), whereas there are few data available of swim speed variation (Calambokidis et al., 2019). Possible options to obtain nighttime movement data include the use of infrared imaging from boats or land stations (Horton, Oline, et al., 2017), or GPS tags that have proven to capture fine-scale movements including swim speeds and dive profiles (Dujon et al., 2014; Meynecke & Liebsch, 2021). Second, it is plausible that the southward flowing EAC influences the swim speed and transit time after whales have negotiated HB leading to overall lower values across this part of the domain compared with the relatively calmer waters before reaching HB. Third, while humpback whales are predominantly surface-oriented during migration and known to display a variety of behaviors, including tail and fin slaps (Kavanagh, Owen, et al., 2017; McCulloch et al., 2021), diving behavior is also part of their migratory movements and influences transit time. Current knowledge regarding factors that induce diving is scarce, but it may facilitate navigation or opportunistic food searching (Henderson et al., 2022) or occur in response to unfavorable conditions at the surface, caused by weather (Kavanagh, Noad, et al., 2017) or human activities (Stamation et al., 2010). The dives themselves are typically executed at an angle with respect to the vertical and include a variable amount of time at the bottom, resulting in different trajectories, such as U- and V-shaped ones (Derville et al., 2020). Despite *eReefs* offering environmental data for 47 vertical layers, extending the current ABM to a fully 3D model would require a distinct set of behavioral rules to accurately reflect diving behavior. Future fieldwork may yield more specific data regarding horizontal and possibly vertical swim speeds that could improve parameter settings to be used for simulations.

For the reasons discussed above, estimations of total transit time between release and the GC also can be improved. In particular, a better understanding of the migratory route taken by southward-migrating whales, which do not enter HB for resting, will provide valuable information on their route selection and decision-making process close to the entrance of the bay, especially in relation to bathymetry. In the ABM, this route is predominantly driven by shallow bathymetry avoidance, which could benefit from validation through satellite tagging of humpback whales. Obtaining such information requires the tagging of individuals shortly after they leave the GBR, which is a time-consuming and costly endeavor. However, such research may further provide information on migratory swim speeds and bouts of resting along the way (Andrews-Goff et al., 2018).

While the spatial domain used in ABM simulations encompasses approximately half of the E1 coastal migratory corridor, it excludes the route taken by the humpback whales after they have passed the GC bay and continue southward until reaching the Eden region. This limitation is due to the spatial domain covered by *eReefs*, which only extends to the New South Wales border (~29°S; Steven et al., 2019). While oceanographic data are readily available (e.g., by the Australian Ocean Data Network), the hourly data provided by the *eReefs* platform are not matched by any other database that also spans the entire East Coast of Australia. This is important for capturing the movements of agents in sufficient detail, especially when migrating close to shorelines and inlets (so that they do not "skip" over them) or where the land avoidance behavior may be activated. Development of a coastal model for east Australia would allow for the ABM to be applied to the entire coastal migratory corridor and validated against tagging data (Andrews-Goff et al., 2018) and/ or citizen science data collected along the route.

In conclusion, the current version of the ABM can capture the migratory movements of the MC cohort of E1 humpback whales and suggests that individuals actively switch direction after passing HB during their southward migration toward feeding grounds. More research is required to improve the model, for instance, by identifying how physiological processes such as respiration and social communication influence swim speed over time and the decision-making process around resting, by understanding how other environmental factors induce behavioral responses that aid their migration, or by providing additional validation data. Future versions of the model could be employed to investigate the effects of climate change on humpback whale migration, for instance, through the EAC warming further south or changes in its path/intensity. While the current ABM is applied to the MC cohort, swim speed data for singletons or pods without a calf have been collected in HB and the GC for many years, allowing future simulation efforts to incorporate these cohorts as well. This would in turn provide a more realistic overview of the entire E1 substock southward migration. Finally, northward migration may also be subject to future simulation efforts and compared to limited data on the movements of northward migrating humpback whales that were satellite-tagged (Gales et al., 2010; Smith et al., 2012), but the development of such an ABM will present new challenges. This includes the influence of the southward flowing EAC that must affect swim speed of the agents, the nonuse of resting areas such as HB, and by extension a lack of validation data on transit times enroute.

ACKNOWLEDGMENTS

The authors wish to thank the Australian Antarctic Division for allowing the usage of satellite tracking data, previously published in Gales et al. (2010) and Smith et al. (2012). This work was supported by a private charitable trust to Griffith University as part of the Whales and Climate Research Program.

AUTHOR CONTRIBUTIONS

Jasper de Bie: Conceptualization; data curation; formal analysis; investigation; software; writing – original draft. **Serena B. Lee:** Methodology; software; visualization; writing – review and editing. **Jan-Olaf Meynecke:** Funding acquisition; methodology; project administration; writing – review and editing. **Elisa Seyboth:** Methodology; writing – review and editing.

Saumik Samanta: Methodology; writing – review and editing. **Marcello Vichi:** Funding acquisition; writing – review and editing. **Alakendra Roychoudhury:** Funding acquisition; writing – review and editing. **Brendan Mackey:** Funding acquisition; writing – review and editing.

Research funding

Private charitable trust supporting Griffith University as part of the Whales & Climate Research Program

REFERENCES

Allen, R. M., Metaxas, A., & Snelgrove, P. V. (2018). Applying movement ecology to marine animals with complex life cycles. *Annual Review of Marine Science*, 10(1), 19–42. https://doi.org/10.1146/annurev-marine-121916-063134

Andrews-Goff, V., Bestley, S., Gales, N. J., Laverick, S. M., Paton, D., Polanowski, A. M., Schmitt, N. T., & Double, M. C. (2018). Humpback whale migrations to Antarctic summer foraging grounds through the southwest Pacific Ocean. *Scientific Reports*, 8(1), 12333. https://doi.org/10.1038/s41598-018-30748-4

Au, W. W., Mobley, J., Burgess, W. C., Lammers, M. O., & Nachtigall, P. E. (2000). Seasonal and diurnal trends of chorusing humpback whales wintering in waters off western Maui. *Marine Mammal Science*, 16(3), 530–544. https://doi.org/10.1111/j.1748-7692.2000.tb00949.x

Baker, C. S., Steel, D., Calambokidis, J., Falcone, E., González-Peral, U., Barlow, J., Burdin, A. M., Clapham, P. J., Ford, J. K., & Gabriele, C. M. (2013). Strong maternal fidelity and natal philopatry shape genetic structure in North Pacific humpback whales. *Marine Ecology Progress Series*, 494, 291–306. https://doi.org/10.3354/meps10508

Beaman, R. (2017). High-resolution depth model for the Great Barrier Reef—30 m (20170025C). *Geoscience Australia, Canberra*. https://doi.org/10.4225/25/5a207b36022d2

Bennett, D. A., & Tang, W. (2006). Modelling adaptive, spatially aware, and mobile agents: Elk migration in Yellowstone. *International Journal of Geographical Information Science*, 20(9), 1039–1066. https://doi.org/10.1080/13658810600830806

Bestley, S., Andrews-Goff, V., Van Wijk, E., Rintoul, S. R., Double, M. C., & How, J. (2019). New insights into prime Southern Ocean forage grounds for thriving Western Australian humpback whales. *Scientific Reports*, 9(1), 1–12. https://doi.org/10.1038/s41598-019-50497-2

Brinkman, R., Wolanski, E., Deleersnijder, E., Mcallister, F., & Skirving, W. (2002). Oceanic inflow from the coral sea into the Great Barrier Reef. *Estuarine, Coastal and Shelf Science*, 54(4), 655–668. https://doi.org/10.1006/ecss.2001.0850

Burns, D., Brooks, L., Harrison, P., Franklin, T., Franklin, W., Paton, D., & Clapham, P. (2014). Migratory movements of individual humpback whales photographed off the eastern coast of Australia. *Marine Mammal Science*, 30(2), 562–578. https://doi.org/10.1111/mms.12057

Calambokidis, J., Fahlbusch, J. A., Szesciorka, A. R., Southall, B. L., Cade, D. E., Friedlaender, A. S., & Goldbogen, J. A. (2019). Differential vulnerability to ship strikes between day and night for blue, fin, and humpback whales based on dive and movement data from medium duration archival tags. *Frontiers in Marine Science*, 6, 543. https://doi.org/10.3389/fmars.2019.00543

Ceccarelli, D. M., Mckinnon, A. D., Andréfouët, S., Allain, V., Young, J., Gledhill, D. C., Flynn, A., Bax, N. J., Beaman, R., & Borsa, P. (2013). The coral sea: Physical environment, ecosystem status and biodiversity assets. In M. Lesser (Ed.), Advances in Marine Biology (pp. 213–290). Elsevier.

Chaloupka, M., Osmond, M., & Kaufman, G. (1999). Estimating seasonal abundance trends and survival probabilities of humpback whales in Hervey Bay (east coast Australia). *Marine Ecology Progress Series*, 184, 291–301. https://doi.org/10.3354/meps184291

Chittleborough, R. (1953). Aerial observations on the humpback whale, *Megaptera nodosa* (Bonnaterre), with notes on other species. *Marine and Freshwater Research*, 4(2), 219–226. https://doi.org/10.1071/MF9530219

Chittleborough, R. (1965). Dynamics of two populations of the humpback whale, *Megaptera novaeangliae* (Borowski). *Marine and Freshwater Research*, 16(1), 33–128. https://doi.org/10.1071/mf9650033

Craig, A. S., Herman, L. M., Gabriele, C. M., & Pack, A. A. (2003). Migratory timing of humpback whales (*Megaptera novaeangliae*) in the central North Pacific varies with age, sex and reproductive status. *Behaviour*, 140(8), 981–1001. https://doi.org/10.1163/156853903322589605

Cusano, D. A., Indeck, K. L., Noad, M. J., & Dunlop, R. A. (2020). Humpback whale (*Megaptera novaeangliae*) social call production reflects both motivational state and arousal. *Bioacoustics*, 31(1), 17–40. https://doi.org/10.1080/09524622.2020.1858450

Dawbin, W. H. (1956). The migrations of humpback whales which pass the New Zealand coast. *Transactions of the Royal Society of New Zealand*, 84(1), 147–196.

Dawbin, W. H. (1966). The seasonal migratory cycle of humpback whales. In K. S. Norris (Ed.), Whales, dolphins and porpoises (pp. 145–170). University of California Press.

Dawbin, W. H. (1997). Temporal segregation of humpback whales during migration in southern hemisphere waters. *Memoirs of the Queensland Museum*, 42, 105–138.

DeAngelis, D. L., & Diaz, S. G. (2019). Decision-making in agent-based modeling: A current review and future prospectus. *Frontiers in Ecology and Evolution*, 6, 237. https://doi.org/10.3389/fevo.2018.00237

Derville, S., Torres, L. G., Iovan, C., & Garrigue, C. (2018). Finding the right fit: Comparative cetacean distribution models using multiple data sources and statistical approaches. *Diversity and Distributions*, 24(11), 1657–1673. https://doi.org/10.1111/ddi.12782

Derville, S., Torres, L. G., Zerbini, A. N., Oremus, M., & Garrigue, C. (2020). Horizontal and vertical movements of humpback whales inform the use of critical pelagic habitats in the western South Pacific. *Scientific Reports*, 10(1), 4871. https://doi.org/10.1038/s41598-020-61771-z

Dodson, S., Abrahms, B., Bograd, S. J., Fiechter, J., & Hazen, E. L. (2020). Disentangling the biotic and abiotic drivers of emergent migratory behavior using individual-based models. *Ecological Modelling*, 432, 109225. https://doi.org/10.1016/j.ecolmodel.2020.109225

Dujon, A. M., Lindstrom, R. T., & Hays, G. C. (2014). The accuracy of Fastloc-GPS locations and implications for animal tracking. *Methods in Ecology and Evolution*, 5(11), 1162–1169. https://doi.org/10.1111/2041-210x.12286

Duriez, O., Bauer, S., Destin, A., Madsen, J., Nolet, B. A., Stillman, R. A., & Klaassen, M. (2009). What decision rules might pink-footed geese use to depart on migration? *An individual-based model. Behavioral Ecology*, 20(3), 560–569. https://doi.org/10.1093/beheco/arp032

Franklin, T., Franklin, W., Brooks, L., & Harrison, P. (2018). Site-specific female-biased sex ratio of humpback whales (*Megaptera novaeangliae*) during a stopover early in the southern migration. *Canadian Journal of Zoology*, 96(6), 533–544. https://doi.org/10.1139/cjz-2017-0086

Franklin, T., Franklin, W., Brooks, L., Harrison, P., Baverstock, P., & Clapham, P. (2011). Seasonal changes in pod characteristics of eastern Australian humpback whales (*Megaptera novaeangliae*), Hervey Bay 1992–2005. *Marine Mammal Science*, 27(3), E134–E152. https://doi.org/10.1111/j.1748-7692.2010.00430.x

Franklin, W., Franklin, T., Gibbs, N., Childerhouse, S., Garrigue, C., Constantine, R., Brooks, L., Burns, D., Paton, D., Poole, M., Hauser, N., Donoghue, M., Russell, K., Mattila, D. K., Robbins, J., Anderson, M., Olavarría, C., Jackson, J., Noad, M., … Clapham, P. (2014). Photo-identification confirms that humpback whales (*Megaptera novaeangliae*) from eastern Australia migrate past New Zealand but indicates low levels of interchange with breeding grounds of Oceania. *Journal of Cetacean Research and Management*, 14(1), 133–140. 10.47536/jcrm.v14i1.530

Friedlaender, A., Tyson, R., Stimpert, A., Read, A., & Nowacek, D. (2013). Extreme diel variation in the feeding behavior of humpback whales along the western Antarctic Peninsula during autumn. *Marine Ecology Progress Series*, 494, 281–289. https://doi.org/10.3354/meps10541

Gales, N., Double, M. C., Robinson, S., Jenner, C., Jenner, M., King, E., Gedamke, J., Childerhouse, S. & Paton, D. (2010). Satellite tracking of Australian humpback (Megaptera novaeangliae) and pygmy blue whales (Balaenoptera musculus brevicauda). White paper

presented to the Scientific Committee of the International Whaling Commission, IWC Morrocco.

Garrigue, C., Clapham, P. J., Geyer, Y., Kennedy, A. S., & Zerbini, A. N. (2015). Satellite tracking reveals novel migratory patterns and the importance of seamounts for endangered South Pacific humpback whales. *Royal Society Open Science*, 2(11), 150489. https://doi.org/10.1098/rsos.150489

Goodwin, R. A., Nestler, J. M., Anderson, J. J., Weber, L. J., & Loucks, D. P. (2006). Forecasting 3-D fish movement behavior using a Eulerian–Lagrangian–agent method (ELAM). *Ecological Modelling*, 192(1), 197–223. https://doi.org/10.1016/j.ecolmodel.2005.08.004

Govekar, P. D., Griffin, C., & Beggs, H. (2022). Multi-sensor sea surface temperature products from the Australian Bureau of Meteorology. *Remote Sensing*, 14(15), 3785. https://doi.org/10.3390/rs14153785

Guarini, J.-M., & Coston-Guarini, J. (2022). A first individual-based model to simulate humpback whale (*Megaptera novaeangliae*) migrations at the scale of the global ocean. *Journal of Marine Science and Engineering*, 10(10), 1412. https://doi.org/10.3390/jmse10101412

Hays, G. C. (2017). Ocean currents and marine life. *Current Biology*, 27(11), R470–R473. https://doi.org/10.1016/j.cub.2017.01.044

Henderson, E. E., Deakos, M., Aschettino, J., Englehaupt, D., & Alongi, G. (2022). Behavior and inter-Island movements of satellite-tagged humpback whales in Hawai'i, USA. *Marine Ecology Progress Series*, 685, 197–213. https://doi.org/10.3354/meps13976

Horton, T. W., Hauser, N., Zerbini, A. N., Francis, M. P., Domeier, M. L., Andriolo, A., Costa, D. P., Robinson, P. W., Duffy, C. A. J., Nasby-Lucas, N., Holdaway, R. N., & Clapham, P. J. (2017). Route fidelity during marine megafauna migration. *Frontiers in Marine Science*, 4, 422. https://doi.org/10.3389/fmars.2017.00422

Horton, T. W., Oline, A., Hauser, N., Khan, T. M., Laute, A., Stoller, A., Tison, K., & Zawar-Reza, P. (2017). Thermal imaging and biometrical thermography of humpback whales. *Frontiers in Marine Science*, 4, 424. https://doi.org/10.3389/fmars.2017.00424

Horton, T. W., Zerbini, A. N., Andriolo, A., Danilewicz, D., & Sucunza, F. (2020). Multi-decadal humpback whale migratory route fidelity despite oceanographic and geomagnetic change. *Frontiers in Marine Science*, 7, 414. https://doi.org/10.3389/fmars.2020.00414

Hunt, K. E., Moore, M. J., Rolland, R. M., Kellar, N. M., Hall, A. J., Kershaw, J., Raverty, S. A., Davis, C. E., Yeates, L. C., Fauquier, D. A., Rowles, T. K., & Kraus, S. D. (2013). Overcoming the challenges of studying conservation physiology in large whales: a review of available methods. *Conservation Physiology*, 1(1), 1–24. https://doi.org/10.1093/conphys/cot006

Johnson, C., Reisinger, R., Friedlaender, A., Palacios, D., Willson, A., Zerbini, A., Lancaster, M., Battle, J., Graham, A., Shahid, U., Houtman, N., Alberini, A., Montecinos, Y., Najera, E., Kelez,

S., & Félix, F. (2022). Protecting Blue Corridors, Challenges and Solutions for Migratory Whales Navigating National and International Seas. WWF International Switzerland.

Kavanagh, A. S., Noad, M. J., Blomberg, S. P., Goldizen, A. W., Kniest, E., Cato, D. H., & Dunlop, R. A. (2017). Factors driving the variability in diving and movement behavior of migrating humpback whales (*Megaptera novaeangliae*): Implications for anthropogenic disturbance studies. *Marine Mammal Science*, 33(2), 413–439. https://doi.org/10.1111/mms.12375

Kavanagh, A. S., Owen, K., Williamson, M. J., Blomberg, S. P., Noad, M. J., Goldizen, A. W., Kniest, E., Cato, D. H., & Dunlop, R. A. (2017). Evidence for the functions of surface-active behaviors in humpback whales (*Megaptera novaeangliae*). *Marine Mammal Science*, 33(1), 313–334. https://doi.org/10.1111/mms.12374

Malan, N., Archer, M., Roughan, M., Cetina-Heredia, P., Hemming, M., Rocha, C., Schaeffer, A., Suthers, I., & Queiroz, E. (2020). Eddy-driven cross-shelf transport in the East Australian Current separation zone. *Journal of Geophysical Research: Oceans*, 125(2), e2019JC015613. https://doi.org/10.1029/2019jc015613

Malan, N., Roughan, M., Stanley, G. J., Holmes, R., & Li, J. (2022). Quantifying cross-shelf transport in the East Australian Current System: A budget-based approach. *Journal of Physical Oceanography*, 52(10), 2555–2572. https://doi.org/10.1175/jpo-d-21-0193.1

McCulloch, S., Meynecke, J.-O., Franklin, T., Franklin, W., & Chauvenet, A. L. M. (2021). Humpback whale (*Megaptera novaeangliae*) behaviour determines habitat use in two Australian bays. *Marine and Freshwater Research*, 72, 1251–1267. https://doi.org/10.1071/MF21065

Meynecke, J.-O., De Bie, J., Menzel Barraqueta, J.-L., Seyboth, E., Prakash Dey, S., Lee, S., Samanta, S., Vichi, M., Findlay, K., Roychoudhury, A., & Mackey, B. (2021). The role of environmental drivers in humpback whale distribution, movement and behaviour: A review. *Frontiers in Marine Science*, 8, 720774. https://doi.org/10.3389/fmars.2021.720774

Meynecke, J.-O., & Liebsch, N. (2021). Asset tracking whales—first deployment of a custom-made GPS/GSM suction cup tag on migrating humpback whales. *Journal of Marine Science and Engineering*, 9(6), 597. https://doi.org/10.3390/jmse9060597

Meynecke, J.-O., Seyboth, E., De Bie, J., Menzel Barraqueta, J.-L., Chama, A., Prakash Dey, S., Lee, S. B., Tulloch, V., Vichi, M., Findlay, K., Roychoudhury, A. N., & Mackey, B. (2020). Responses of humpback whales to a changing climate in the Southern Hemisphere: Priorities for research efforts. *Marine Ecology*, 41(6), e12616. https://doi.org/10.1111/maec.12616

Noad, M. J., & Cato, D. H. (2007). Swimming speeds of singing and non-singing humpback whales during migration. *Marine Mammal Science*, 23(3), 481–495.

Nowacek, D. P., Christiansen, F., Bejder, L., Goldbogen, J. A., & Friedlaender, A. S. (2016). Studying cetacean behaviour: New technological approaches and conservation applications. *Animal Behaviour*, 120, 235–244. https://doi.org/10.1016/j.anbehav.2016.07.019

Oke, P. R., Roughan, M., Cetina-Heredia, P., Pilo, G. S., Ridgway, K. R., Rykova, T., Archer, M. R., Coleman, R. C., Kerry, C. G., & Rocha, C. (2019). Revisiting the circulation of the East Australian Current: Its path, separation, and eddy field. *Progress in Oceanography*, 176, 102139. https://doi.org/10.1016/j.pocean.2019.102139

Parks, S. E., Cusano, D. A., Stimpert, A. K., Weinrich, M. T., Friedlaender, A. S., & Wiley, D. N. (2014). Evidence for acoustic communication among bottom foraging humpback whales. *Scientific Reports*, 4(1), 7508. https://doi.org/10.1038/srep07508

Ransome, N., Kew, A., Duque, E., Morais, M., Wright, W., & Smith, J. N. (2022). Escorting of a mother humpback whale (*Megaptera novaeangliae*) and the death of her calf during aggressive mating behavior. *Marine Mammal Science*, 38(4), 1643–1653. https://doi.org/10.1111/mms.12922

Rasmussen, K., Palacios, D. M., Calambokidis, J., Saborío, M. T., Dalla Rosa, L., Secchi, E. R., Steiger, G. H., Allen, J. M., & Stone, G. S. (2007). Southern Hemisphere humpback whales wintering off Central America: Insights from water temperature into the longest mammalian migration. *Biology Letters*, 3(3), 302–305. https://doi.org/10.1098/rsbl.2007.0067

Reinke, J., Lemckert, C., & Meynecke, J.-O. (2016). Coastal fronts utilized by migrating humpback whales, *Megaptera novaeangliae*, on the Gold Coast, Australia. *Journal of Coastal Research*, 75, 552–557. https://doi.org/10.2112/si75-111.1

Ridgway, K., & Dunn, J. (2003). Mesoscale structure of the mean East Australian Current System and its relationship with topography. *Progress in Oceanography*, 56(2), 189–222. https://doi.org/10.1016/s0079-6611(03)00004-1

Riekkola, L., Zerbini, A. N., Andrews, O., Andrews-Goff, V., Baker, C. S., Chandler, D., Childerhouse, S., Clapham, P., Dodémont, R., Donnelly, D., Friedlaender, A., Gallego, R., Garrigue, C., Ivashchenko, Y., Jarman, S., Lindsay, R., Pallin, L., Robbins, J., Steel, D., … Constantine, R. (2018). Application of a multi-disciplinary approach to reveal population structure and Southern Ocean feeding grounds of humpback whales. *Ecological Indicators*, 89, 455–465. https://doi.org/10.1016/j.ecolind.2018.02.030

Ross-Marsh, E., Elwen, S. H., Prinsloo, A., James, B., & Gridley, T. (2021). Singing in South Africa: Monitoring the occurrence of humpback whale (*Megaptera novaeangliae*) song near the Western Cape. *Bioacoustics*, 30(2), 163–179. https://doi.org/10.1080/09524622.2019.1710254

Schmitt, N. T., Double, M. C., Jarman, S. N., Gales, N., Marthick, J. R., Polanowski, A. M., Scott Baker, C., Steel, D., Jenner, K. C. S., Jenner, M. N., Gales, R., Paton, D., & Peakall, R. (2014). Low levels of genetic differentiation characterize Australian humpback whale (*Megaptera novaeangliae*) populations. *Marine Mammal Science*, 30(1), 221–241. https://doi.org/10.1111/mms.12045

Shabangu, F. W., & Kowarski, K. A. (2022). The beat goes on: humpback whale song seasonality in Antarctic and South African waters. *Frontiers in Marine Science*, 9, 827324. https://doi.org/10.3389/fmars.2022.827324

Shaw, A. K. (2016). Drivers of animal migration and implications in changing environments. *Evolutionary Ecology*, 30(6), 991–1007. https://doi.org/10.1007/s10682-016-9860-5

Smith, J. N., Grantham, H. S., Gales, N., Double, M. C., Noad, M. J., & Paton, D. (2012). Identification of humpback whale breeding and calving habitat in the Great Barrier Reef. *Marine Ecology Progress Series*, 447, 259–272. https://doi.org/10.3354/meps09462

Stamation, K. A., Croft, D. B., Shaughnessy, P. D., Waples, K. A., & Briggs, S. V. (2010). Behavioral responses of humpback whales (*Megaptera novaeangliae*) to whale-watching vessels on the southeastern coast of Australia. *Marine Mammal Science*, 26(1), 98–122.

Steven, A. D., Baird, M. E., Brinkman, R., Car, N. J., Cox, S. J., Herzfeld, M., Hodge, J., Jones, E., King, E., Margvelashvili, N., Robillot, C., Robson, B., Schroeder, T., Skerratt, J., Tickell, S., Tuteja, N., Wild-Allen, K., & Yu, J. (2019). eReefs: an operational information system for managing the Great Barrier Reef. *Journal of Operational Oceanography*, 12(sup2), S12–S28. https://doi.org/10.1080/1755876x.2019.1650589

Stevick, P. T., Allen, J., Bérubé, M., Clapham, P. J., Katona, S. K., Larsen, F., Lien, J., Mattila, D. K., Palsbøll, P. J., & Robbins, J. (2003). Segregation of migration by feeding ground origin in North Atlantic humpback whales (*Megaptera novaeangliae*). *Journal of Zoology*, 259(3), 231–237. https://doi.org/10.1017/s0952836902003151

Suthers, I. M., Young, J. W., Baird, M. E., Roughan, M., Everett, J. D., Brassington, G. B., Byrne, M., Condie, S. A., Hartog, J. R., Hassler, C. S., Hobday, A. J., Holbrook, N. J., Malcolm, H. A., Oke, P. R., Thompson, P. A., & Ridgway, K. (2011). The strengthening East Australian current, its eddies and biological effects—an introduction and overview. *Deep-Sea Research II*, 58, 538–546. https://doi.org/10.1016/j.dsr2.2010.09.029

Torre-Williams, L., Martinez, E., Meynecke, J., Reinke, J., & Stockin, K. (2019). Presence of newborn humpback whale (*Megaptera novaeangliae*) calves in Gold Coast Bay, Australia. *Marine and Freshwater Behaviour and Physiology*, 52(5), 199–216.

Tulloch, V. J., Plagányi, É. E., Brown, C., Richardson, A. J., & Matear, R. (2019). Future recovery of baleen whales is imperiled by climate change. *Global change biology*, 25(4), 1263–1281. https://doi.org/10.1111/gcb.14573

Valani, R., Meynecke, J.-O., & Olsen, M. T. (2020). Presence and movement of humpback whale (*Megaptera novaeangliae*) mother-calf pairs in the Gold Coast, Australia. *Marine and Freshwater Behaviour and Physiology*, 53(5-6), 251–263. https://doi.org/10.1080/10236244.2020.1850177

Viddi, F. A., Hucke-Gaete, R., Torres-Florez, J. P., & Ribeiro, S. (2010). Spatial and seasonal variability in cetacean distribution in the fjords of northern Patagonia, Chile. *ICES Journal of Marine Science*, 67(5), 959–970. https://doi.org/10.1093/icesjms/fsp288

Wilson, L. J., Fulton, C. J., Hogg, A. M., Joyce, K. E., Radford, B. T., & Fraser, C. I. (2016). Climate-driven changes to ocean circulation and their inferred impacts on marine dispersal patterns. *Global Ecology and Biogeography*, 25(8), 923–939. https://doi.org/10.1111/geb.12456

Xie, S., Huang, Z., & Wang, X. H. (2021). Remotely sensed seasonal shoreward intrusion of the East Australian Current: Implications for coastal ocean dynamics. *Remote Sensing*, 13(5), 854. https://doi.org/10.3390/rs13050854